



Frustrated spin-1/2 dimer compound $K_2Co_2(SeO_3)_3$ with easy-axis anisotropyRuidan Zhong,^{*} Shu Guo, Loi T. Nguyen , and Robert J. Cava[†]
Department of Chemistry, Princeton University, Princeton, New Jersey 08544, USA (Received 2 September 2020; revised 30 November 2020; accepted 8 December 2020; published 24 December 2020)

Magnetic susceptibility, magnetization, and specific-heat measurements under both in-plane and out-of-plane field on $K_2Co_2(SeO_3)_3$ single crystals are reported. The Co dimers in this compound, which are made from face-sharing effective spin-1/2 CoO_6 octahedra, sit on the corners of a geometrically frustrating triangular planar lattice. No long-range magnetic ordering is found down to 0.35 K, which, together with the large negative Curie-Weiss temperature obtained from fitting the temperature-dependent magnetic susceptibility, indicates that the system is magnetically frustrated. Analysis of the field and orientation dependence of the magnetic and thermodynamic properties suggests the presence of an easy-axis anisotropy. The magnetic fluctuations present due to geometric frustration are more resistant to an in-plane field than a perpendicular-to-plane field.

DOI: [10.1103/PhysRevB.102.224430](https://doi.org/10.1103/PhysRevB.102.224430)**I. INTRODUCTION**

Spin-dimer systems are currently the subjects of intense theoretical and experimental investigation due to the fact that their magnetic interactions can provide access to novel low-temperature states [1,2]. Dimer systems feature intrinsically strong antiferromagnetic (AFM) intradimer spin-spin interactions, such that at zero applied field the ground state is expected to be a singlet ($S = 0$)—the building block for an overall nonmagnetic ground state that, in the absence of further coupling, does not show long-range magnetic ordering down to zero temperature [3,4]. The singlet ground state formed by static valence bonds in dimer systems is a valence-bond solid, and has been confirmed in several materials [5–7]. In contrast, in recent years, particular attention has been paid to singlets made from dynamic valence bonds, or the resonating valence-bond state, believed by many to underlie the physics of high-temperature superconductivity and quantum spin liquids [8]. Such quantum states are preferred in systems with low spin and magnetic frustration. Strong geometric frustration sustains quantum fluctuations and typically gives rise to degeneracy that favors a spin liquid magnetic ground state [4,9]. It is thus of interest to study materials based on a geometrically frustrated triangular planar lattice decorated by perpendicular-to-plane singlet-bearing spin dimers. Such frustrated spin-dimer systems have been realized, for example, in compounds with the general formula $A_3M_2O_8$, where A is Ba or Sr, and M is a $5+3d$ transition metal like Cr or Mn [10–12]. Singlet ground states in those frustrated dimer systems have been confirmed experimentally [11,13,14], evidenced by a lack of long-range magnetic ordering, by a sharp decrease in susceptibility, and by magnetization plateaus in $M(H)$.

In most real triangular lattice materials, nevertheless, the spin liquid state and geometric frustration can be bypassed through the formation of a 120° noncollinear spin structure, for XY and Heisenberg antiferromagnets, resulting in a long-range ordered phase [15]. In contrast, Ising antiferromagnets on a triangular lattice are of interest for their relative simplicity, and the fact that they can realize a spin liquid phase through geometric frustration [16]. Ising spins can be present in real materials when the spins have a strong easy-axis anisotropy; magnetic anisotropy indicates that the spins have a preferred axial orientation in the absence of an applied field. Typically, if the spins are aligned along a well-defined axis, either parallel or antiparallel, then the system is usually classified as an *easy-axis* system; if the spins are confined in a plane, then the system is categorized as *easy plane*. Therefore, triangular antiferromagnets such as the Yb-112 compound [17], which displays easy-plane anisotropy, appear to fall into the category of Heisenberg magnets, while, when easy-axis anisotropy is observed in systems, the spins are likely to be Ising like.

The result of a mild hydrothermal reaction [18], the existence and crystal structure of $K_2Co_2(SeO_3)_3$ were first reported in 1994. Inspection of the reported crystal structure and atomic makeup of this compound reveals that it is a magnetic system based on dimers of $S = 1/2$, $3d^7$ Co^{2+} ions arranged on a triangular planar lattice, serving as an extension to the current frustrated spin-dimer systems. The single crystals obtained hydrothermally, however, are too small to be suitable for magnetic characterization. Here we report a crystal growth method for $K_2Co_2(SeO_3)_3$ that yields crystals suitable for investigation by means of orientation-dependent magnetic susceptibility, magnetization, and specific-heat studies. We find that $K_2Co_2(SeO_3)_2$ is a strongly frustrated magnet that displays easy-axis anisotropy. Moreover, we observe several magnetic characteristics that are common in spin-dimer systems, such as a broad transition in susceptibility with no indication of three-dimensional long-range ordering down to 0.35 K, and a magnetization plateau in the intermediate field region. Finally, we find that the dimer spins are less affected by an in-plane magnetic field than a perpendicular-to-plane field.

^{*}Current address: Tsung-Dao Lee Institute & School of Physics and Astronomy, Shanghai Jiao Tong University, Shanghai 200240, China.

[†]rcava@princeton.edu

II. METHODS

Single crystals of $\text{K}_2\text{Co}_2(\text{SeO}_3)_3$ were synthesized via solid-state reaction. Due to the volatility of carbonates and the toxicity of selenium dioxide, dried K_2CO_3 (99%), CoO (99%), and SeO_2 (99.9%) were mixed sealed in an evacuated quartz glass tube with an optimal molar ratio of 1.3:2:3.2. The ampoule was heated to 600 °C, held for 8 h, and then cooled to room temperature in 8 h. The magenta color single crystals were readily detached from the quartz tube wall by dissolving the product in distilled water. The obtained single crystals are stable in air and moisture.

The crystal structure of $\text{K}_2\text{Co}_2(\text{SeO}_3)_3$ at 100(1) K was determined by single-crystal x-ray diffraction. The diffraction data were collected on a single crystal with a Kappa Apex2 charge-coupled device diffractometer (Bruker) using graphite-monochromated $\text{Mo-K}\alpha$ radiation ($\lambda = 0.710\ 73\ \text{\AA}$). The raw data were corrected for background, polarization, and Lorentz factors and multiscan absorption corrections were applied. Finally, the structure was analyzed by the Intrinsic Phasing method provided by the SHELXT structure solution program [19] and refined using the SHELXL least-squares refinement package with the OLEX2 program [20]. The ADDSYM algorithm in the program PLATON was used to double check for possible higher symmetry [21]. The purity of the crushed single crystals was examined by powder x-ray diffraction on a Bruker D8 Advance Eco instrument with $\text{Cu K}\alpha$ radiation ($\lambda = 1.5406\ \text{\AA}$) at room temperature.

Both magnetization and specific-heat measurements were performed using a Dynacool Quantum Design Physical Property Measurement System. Anisotropic magnetization from 1.8 to 300 K was measured using the vibrating sample magnetometer function within the range of magnetic fields of -9 to 9 T. Single crystals were mounted with GE varnish in two orientations, $H||ab$ or $H||c$, on a silica sample holder. The applied field for the temperature-dependent magnetic susceptibility $\chi(T)$ was $H = 1\ \text{kOe}$, where χ is defined as M/H . Specific-heat data were collected down to 0.35 K under both in-plane and out-of-plane applied magnetic fields.

III. RESULTS AND DISCUSSION

A. Crystal structure

The crystal structure of $\text{K}_2\text{Co}_2(\text{SeO}_3)_3$ measured at 100 K is schematically shown in Figs. 1(a) and 1(b). The crystal structure differs only in detail from what has previously been reported for 300 K [18]. Quantitative crystal structure information at 100 K is given in the Supplemental Material [22]. $\text{K}_2\text{Co}_2(\text{SeO}_3)_3$ crystallizes in the centrosymmetric hexagonal space group $P6_3/mmc$, No. 194, with unit cell $a = b = 5.4715(7)\ \text{\AA}$ and $c = 17.510(3)\ \text{\AA}$. There are two layers per unit cell, stacked along c , and thus there are two dimers in each unit cell. The structural refinement shows that the K, Co, and Se1 atoms each fully occupy a single crystallographic position. The O atoms also fully occupy well-defined positions ($6h$ and $12k$). However, the Se2 atoms, on the Wyckoff position $4f$, split into two sites with half-half occupancy, resulting in minor structural disorder within the structure. Tests to determine whether there is a superstructure present

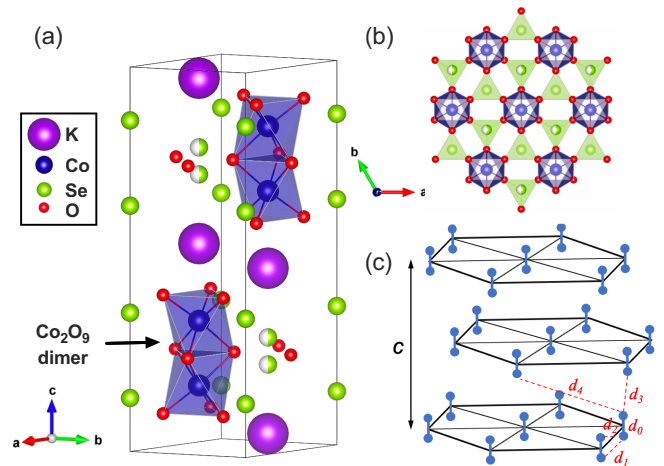


FIG. 1. (a) The crystal structure of $\text{K}_2\text{Co}_2(\text{SeO}_3)_3$ is constructed from two layers of Co_2O_9 dimers, shown in blue polyhedra. The half-colored Se(II) sites display half-half occupancy, while the Se(I) sites, which join the Co_2O_9 dimers in the plane, are fully occupied. (b) Projection of the triangular lattice on the ab plane. The adjacent Co dimers are connected via Se(I)O_3 tripods. (c) Schematic diagram of the crystal structure of $\text{K}_2\text{Co}_2(\text{SeO}_3)_3$ showing the hexagonal network together with the Co^{2+} spin dimers (pairs of blue spheres) in the ab plane. The stacking of the triangular planes along the c axis is an $ABAB$ arrangement. The Co-Co distances within a dimer d_0 (2.94 Å), between the intraplane adjacent dimer d_1 (5.47 Å), d_2 (6.21 Å), and between two dimers in adjacent planes d_3 (6.61 Å) and d_4 (8.58 Å) are shown in the plot.

for this material that would indicate full site-empty site Se2 ordering schemes (i.e. one site completely full and another site completely empty, averaging out to half occupancy in the unit cell and space group employed), were negative, and the crystallographic E -value statistics ($|E^2 - 1|$) obtained, 0.98, is close to the theoretically expected value for a centrosymmetric space group (0.97). Thus, the random distribution of Se2 on two equivalent sites within the centrosymmetric space group is confirmed. It can be assumed that over a short range (say, over a few unit cells) the occupancy of one or the other of the two possible Se2 sites is random. Due to the strong tripodlike shape of the Se-O_3 coordination polyhedron, required by the Se lone pair, the disorder will be static rather than dynamic.

The magnetic part of the $\text{K}_2\text{Co}_2(\text{SeO}_3)_3$ crystal structure is based on triangular planes of Co_2O_9 dimers, formed by pairs of face-sharing CoO_6 octahedra. The dimers are oriented perpendicular to the hexagonal basal plane. The two Co atoms in the Co_2O_9 dimers are quite close, with a separation of 2.96 Å. This is indicative of strong magnetic interactions within the dimer. Within the triangular plane [Fig. 1(b)], adjacent Co_2O_9 dimers are connected to each other through the Se(I)O_3 tripods, and therefore there is no disorder in their in-plane coupling. Each Co dimer has six nearest-neighbor in-plane dimers; the dimers are separated in plane by 5.49 Å. K atoms reside between the planes of magnetic dimers. The dimers are stacked in an $A-B-A-B$ stacking sequence along the c axis. No disorder is present on the magnetic ion site. A schematic view of the arrangement of the Co_2O_9 dimers in $\text{K}_2\text{Co}_2(\text{SeO}_3)_3$ is shown in Fig. 1(c). Unlike the well-studied

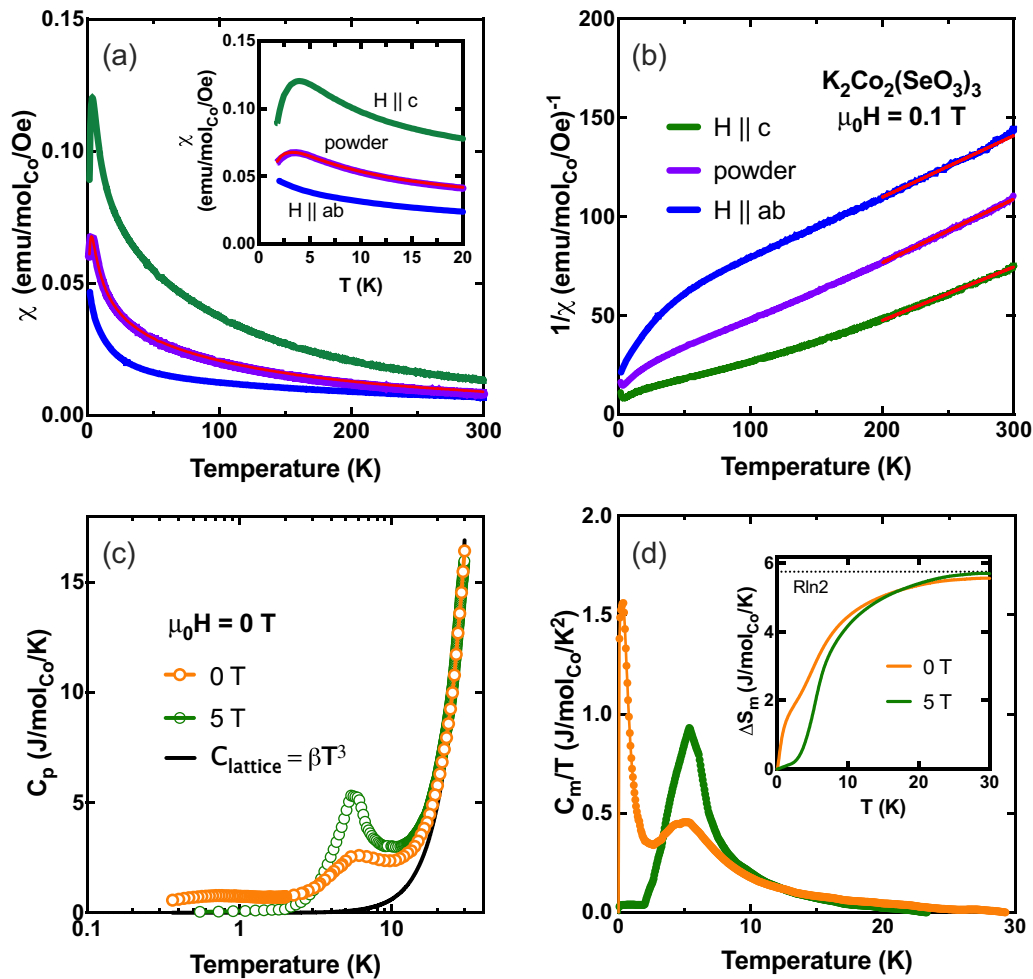


FIG. 2. (a) Anisotropic magnetic susceptibility of $\text{K}_2\text{Co}_2(\text{SeO}_3)_3$ measured on single crystal and polycrystalline samples at 0.1 T. The calculated average magnetic susceptibility is plotted in red, overlapping with the measured susceptibility of polycrystalline powder. Inset shows an expanded view of the broad transition at 4.5 K. (b) Inverse magnetic susceptibility $1/\chi(T)$ measured at 0.1 T. The red lines on the inverse susceptibility represent the Curie-Weiss fitting between 200 and 300 K. (c) Total specific heat as a function of temperature for $\text{K}_2\text{Co}_2(\text{SeO}_3)_3$ shown in logarithmic scale, measured under 0 and 5 T. The black curve illustrates the fit to the phonon contribution to the total specific heat. (d) Temperature dependence of the magnetic specific heat divided by temperature, C_m/T . Inset shows the calculated magnetic entropy as a function of temperature. The dashed line indicates the value of $R\ln 2$.

triangular-lattice dimer compound $\text{Ba}_3\text{Mn}_2\text{O}_8$ in which the interbilayer exchange couplings are significant due to short Mn-Mn interlayer distance [12], the intraplane interactions are dominating in $\text{K}_2\text{Co}_2(\text{SeO}_3)_3$ because of a shorter distance between the dimers within the plane (i.e., d_1 and d_2 are shorter than d_3 and d_4), leading to a quasi-two-dimensional (quasi-2D) triangular plane with substantial geometrical frustration.

B. Strongly frustrated magnetism

While the spin state of $\text{Co}^{2+}(3d^7)$ usually adopts a high spin state ($S = 3/2$) in the high-temperature region, Co^{2+} is a Kramers doublet ion and the effective moment can be described as spin-1/2 at low temperature due to the presence of strong spin-orbit coupling (SOC) and low-symmetric crystal field [23–26]. Figures 2(a) and 2(b) show the temperature dependence of the magnetic susceptibility of single-crystal $\text{K}_2\text{Co}_2(\text{SeO}_3)_3$, measured for fields applied in the ab plane and along the c axis. The magnetic characterization of a

polycrystalline powder sample is also shown. As shown in the inset of Fig. 2(a), for $H\parallel c$, i.e., parallel to the dimers, no sharp transition characteristic of a three-dimensional ordering transition is seen in χ_{\parallel} ; a broad maximum near 5 K is apparent, however, reflecting the presence of short-range magnetic order below this temperature. Below 5 K $\chi_{\parallel}(T)$ decreases rapidly, which is a characteristic feature in spin-dimer materials and indicates the opening of a spin gap [11,13,27,28]. A Curie-Weiss (CW) fit to the high-temperature ($T \geq 200$ K) susceptibility in the paramagnetic state yields a positive Curie-Weiss temperature, $\Theta_{\parallel} = 17.1$ K, and an effective moment of $\mu_{\text{eff},\parallel} = 5.5\mu_B/\text{Co}$. When the applied field is within the plane, i.e., perpendicular to the c axis, the system shows neither long-range ordering down to 1.8 K in χ_{\perp} . A large negative CW temperature of $\Theta_{\perp} = -143.2$ K and an effective moment of $\mu_{\text{eff},\perp} = 5.0\mu_B/\text{Co}$ are derived from the fitting, indicative of strong AFM interactions within the triangular lattice. The magnetic susceptibility of the powder sample yields the averaged behavior, giving rise to the CW fitting parameters

of $\Theta_p = -44.0$ K and $\mu_{\text{eff},p} = 5.1 \mu_B/\text{Co}$. The red curve in Fig. 2(a) shows the average magnetic susceptibility $\bar{\chi}$ of the single crystal given by $\bar{\chi} = 1/3\chi_{\parallel} + 2/3\chi_{\perp}$. The calculated value matches well with the measured susceptibility of the powder. It is worth noticing that the effective moment for each dimerized spin is comparable to that in isolated Co systems [29,30], ruling out the formation of the covalent bonds that strongly suppress the magnetism in other transition-metal dimer systems [31].

The zero-field specific-heat $C_p(T)$ of a $\text{K}_2\text{Co}_2(\text{SeO}_3)_3$ single crystal is displayed in Fig. 2(c). At zero field, no λ peak, associated with long-range magnetic ordering, can be observed down to 0.35 K. There is finite specific heat below 2 K, which points to a possible spin liquid low-temperature state. The lack of a magnetic ordering transition down to the lowest measuring temperature, 0.35 K, yields the empirical frustration parameter $f = \frac{|\Theta_p|}{T_N} > 126$ for $\text{K}_2\text{Co}_2(\text{SeO}_3)_3$, suggesting that it is a strongly frustrated magnetic system. A broad maximum is observed near 5 K, however, consistent with the temperature where a broad transition is found in $\chi_{\parallel}(T)$. A similar feature observed in the spin-dimer compound $\text{Sr}_3\text{Cr}_2\text{O}_8$ has been attributed to the presence of a spin gap between a singlet ground state and excited triplet states [13]. After applying an external field of 5 T, the specific heat shows a broad peak around 5 K then approaches zero at lower temperatures.

Since a nonmagnetic isostructural reference is not available, we use the equation $C_{\text{lattice}}(T) = \beta T^3$ to roughly fit the specific-heat data in the temperature region above 20 K, shown in Fig. 2(c), and estimate the magnetic specific heat. The conventional conduction electron contribution $C_{el}(T) = \gamma T$ to the specific heat is negligible at low temperature in a nonmagnetic compound with low carrier density. Thus the $C_p(T)$ for a nonmagnetic analog will be dominated by a phonon contribution $C_{\text{lattice}}(T)$, which obeys the Debye- T^3 power law in this temperature range. Fitting of this formula to the experimental data between 20 and 30 K yields a Debye temperature $\Theta_D \cong 146.5$ K. The magnetic contribution $C_m(T)$ to the specific heat can then be obtained by subtracting the estimated lattice contribution $C_{\text{lattice}}(T)$ from the observed specific heat. The result is plotted as $C_m(T)/T$ vs T in Fig. 2(d) in zero field. Despite the anomaly near 5 K, an upturn is present at low temperatures. Any potential nuclear contribution from Co or the other atoms present is insignificant in this temperature range due to the small hyperfine field—and thus the contribution of nuclear states to the total specific heat is at least two orders of magnitude lower than what is observed here [32]. Thus, the upturn at low temperatures appears to be an intrinsic feature, arising from the magnetic spins in this system. A similar upturning feature observed in a Co-based triangular lattice compound has been considered as an outcome of dynamic spin fluctuations [29,33]. After subtracting $C_{\text{lattice}}(T)$ from the total specific heat and assuming an extrapolation to 0 K below the lowest measured temperature of 0.35 K, we calculated the total magnetic entropy $S_m(T)$ by integrating the magnetic contribution $C_m(T)/T$ from $T = 0$ to 30 K. As shown in Fig. 2(d), at $T \sim 30$ K, the total entropy for both fields reaches almost $R \ln 2 = 5.76$ J/mol/K, as expected for an effective spin-1/2 state or a two-state Ising system. The significant increment in total entropy near 5 K reflects

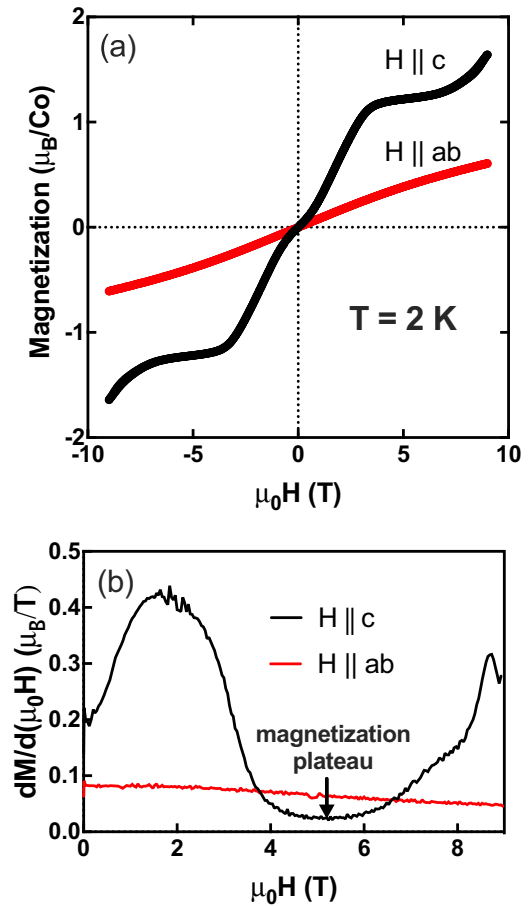


FIG. 3. (a) Magnetic field dependence of magnetization of $\text{K}_2\text{Co}_2(\text{SeO}_3)_2$ single crystals with the field parallel to the crystallographic c axis and ab plane at base temperature. (b) Differential of magnetization as a function of field. A magnetization plateau is evident between 4 and 6 T.

short-range magnetic ordering, perhaps of the Co spins within the dimers.

C. Easy-axis anisotropy

The magnetic anisotropy of single crystal of $\text{K}_2\text{Co}_2(\text{SeO}_3)_3$ was determined by measuring the isothermal magnetization $M(H)$. Figure 3(a) shows the hysteresis loop measured both in $(H \parallel ab)$ and perpendicular to the triangular basal plane $(H \parallel c)$ at 2 K. No magnetic hysteresis can be observed for either direction. At 2 K, a metamagnetic transition is seen for $(H \parallel c)$, with a magnetization plateau present in the applied field region near 4–6 T [Fig. 3(b)]. In the plateau, a saturated moment of $1.2 \mu_B/\text{Co}$ is observed. With increasing applied field, the magnetization increases but does not saturate up to 9 T. Magnetization plateaus are quite common in frustrated magnets, corresponding to different spontaneous broken symmetries [34]. Since here we are not able to achieve lower temperature and obtain a full saturation moment due to a lack of high-field magnetization data, the origin of this magnetization plateau remains unclear and requires further investigation. There are experimental observations of successive magnetization plateaus in the

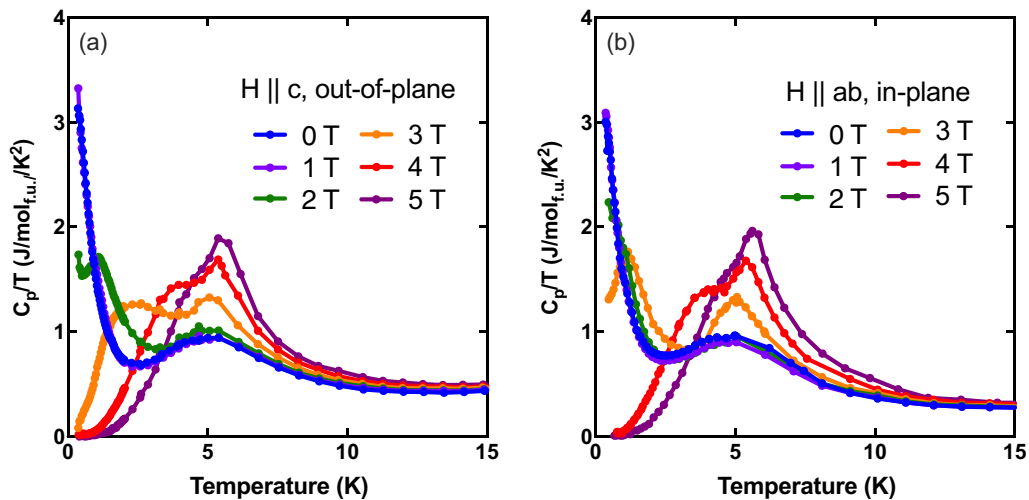


FIG. 4. The temperature-dependent total specific heat of $\text{K}_2\text{Co}_2(\text{SeO}_3)_3$ measured at various applied magnetic fields, with $H||c$ (a) and $H||ab$ (b).

quasi-2D dimer compound $\text{SrCu}_2(\text{BO}_3)_2$ or the frustrated spin-dimer system $\text{Ba}_3\text{Mn}_2\text{O}_8$, in which such magnetization plateaus have been attributed to the successive formation of different spin superlattices [35,36] or the field-induced condensation of a triplet state [37,38].

In the case of $H||ab$, the magnetization increases monotonically with applied field without any features. The linear field dependence of $H||ab$ is consistent with a continuous spin reorientation when the applied field rotates the moment to be aligned with the plane. Compared to the other field orientation, the magnetization changes less with field for $H||ab$, and is far from saturation at 9 T. Although the magnetic anisotropy of Co^{2+} contains a significant contribution from the SOC, the metamagnetization together with the large magnetic moment when the field is applied along the c axis indicate that a large easy-axis anisotropy is present in the layered compound $\text{K}_2\text{Co}_2(\text{SeO}_3)_3$.

We also investigated the specific heat under both in-plane and out-of-plane field, which provides another view on the anisotropic magnetization. As shown in Fig. 4(a), for external field applied along the easy axis, i.e., the c axis, the specific-heat C_p/T exhibits a broad maximum around 5 K together with an upturn at lower temperatures, indicative of the presence of large magnetic entropy. With increasing field, the high-temperature hump gets enhanced in intensity and shifts to slightly higher temperatures. In contrast, the low-temperature upturn remains unaffected below 2 T, and then evolves into a Schottky-type anomaly with its center moving to higher temperatures until it merges with the high-temperature hump. The origin of such a heat capacity anomaly is complicated by its insensitivity to low magnetic fields, calling for further investigation. In Fig. 4(b), the field effect displays similar trend for $H||ab$ despite that the low-temperature upturn evolves into a conventional broad peak until 3 T. Thus, it can be speculated that the high-temperature hump is associated with an intrinsic bulk property that is insensitive to the field direction in this field and temperature range, presumably related to the short-range magnetic ordering. In contrast, the upturning feature below 2 K suggests

large magnetic entropy due to quantum fluctuations, which are a consequence of the strong magnetic frustration within the triangular plane. Thus, when the field is applied along the easy axis and suppresses the intraplane antiferromagnetic interactions between Co moments, such quantum fluctuations due to geometric frustration get disrupted and the system develops into a conventional short-range correlated state. Similarly, since the spins are more resistant to the in-plane field, the quantum fluctuations survive until larger field.

IV. CONCLUSIONS

In conclusion, we have investigated the magnetic and thermodynamic properties of a Co dimer-based compound, $\text{K}_2\text{Co}_2(\text{SeO}_3)_3$, under a magnetic field applied both perpendicular ($H||c$) and parallel ($H||ab$) to the triangular plane. The magnetic dimers are made of face-sharing Co octahedra and sit on triangular plane. Strong intralayer antiferromagnetic interactions between Co moments are derived from the large negative Curie-Weiss temperature $\Theta_{\perp} = 143.2$ K. Together with the fact that no long-range magnetic ordering is detected down to 0.35 K, we expect the strong magnetic frustration within the triangular plane. Characteristic features of spin-dimer systems are observed in $\chi_{||}$, with a broad transition near 5 K and a sudden drop in susceptibility below that temperature. The zero-field magnetic specific heat shows a broad hump near 5 K, which we speculate is due to the short-range magnetic correlations that are associated with the formation of the singlet state in the dimers. At a temperature below 2 K, a significant enhancement is observed in the magnetic specific heat. We propose that the large magnetic entropy present at low temperature is a result of strong quantum fluctuations due to geometric frustration. Both magnetization and specific-heat measurements show a field-orientation dependence that points to an easy-axis anisotropy in $\text{K}_2\text{Co}_2(\text{SeO}_3)_3$. For magnetic field applied along the c axis, a metamagnetic transition is observed, with a magnetization plateau clearly present at 2 K. The intermediate spin structure in this state is stable enough to resist to the thermal effects present at 2 K.

In addition, the field orientation has a direct impact on the magnetic frustration. Since the Co spins are more resistant to a perpendicular field, i.e., a field applied in the plane, quantum fluctuations result from the geometric frustration are less likely to be affected so that a spin liquid ground state can be preserved up to higher field. We hope that further experimental work on three-dimensional spin-dimer system on triangular lattice will be of interest.

ACKNOWLEDGMENTS

The material synthesis, crystal structure determination, and physical properties characterizations were supported as part of the Institute for Quantum Matter, an Energy Frontier Research Center funded by the US Department of Energy, Office of Science, Basic Energy Sciences under Award No. DE-SC0019331.

-
- [1] T. M. Rice, To condense or not to condense, *Science* **298**, 760 (2002).
- [2] S. E. Sebastian, N. Harrison, C. D. Batista, L. Balicas, M. Jaime, P. A. Sharma, N. Kawashima, and I. R. Fisher, Dimensional reduction at a quantum critical point, *Nature (London)* **441**, 617 (2006).
- [3] M. Matsumoto, T. Shoji, and M. Koga, Theory of magnetic excitations and electron spin resonance for anisotropic spin dimer systems, *J. Phys. Soc. Jpn.* **77**, 074712 (2008).
- [4] L. Balents, Spin liquids in frustrated magnets, *Nature (London)* **464**, 199 (2010).
- [5] H. Iwase, M. Isobe, Y. Ueda, and H. Yasuoka, Observation of spin gap in CaV_2O_5 by NMR, *J. Phys. Soc. Jpn.* **65**, 2397 (1996).
- [6] H. Kageyama, K. Yoshimura, R. Stern, N. V. Mushnikov, K. Onizuka, M. Kato, K. Kosuge, C. P. Slichter, T. Goto, and Y. Ueda, Exact Dimer Ground State and Quantized Magnetization Plateaus in the Two-Dimensional Spin System $\text{SrCu}_2(\text{BO}_3)_2$, *Phys. Rev. Lett.* **82**, 3168 (1999).
- [7] W. Shiramura, K. Takatsu, H. Tanaka, K. Kamishima, M. Takahashi, H. Mitamura, and T. Goto, High-field magnetization processes of double spin chain systems KCuCl_3 and TlCuCl_3 , *J. Phys. Soc. Jpn.* **66**, 1900 (1997).
- [8] P. W. Anderson, The resonating valence bond state in La_2CuO_4 and superconductivity, *Science* **235**, 1196 (1987).
- [9] R. Moessner, Magnets with strong geometric frustration, *Can. J. Phys.* **79**, 1283 (2001).
- [10] M. Kofu, J.-H. Kim, S. Ji, S.-H. Lee, H. Ueda, Y. Qiu, H.-J. Kang, M. A. Green, and Y. Ueda, Weakly Coupled $s = 1/2$ Quantum Spin Singlets in $\text{Ba}_3\text{Cr}_2\text{O}_8$, *Phys. Rev. Lett.* **102**, 037206 (2009).
- [11] M. Uchida, H. Tanaka, M. I. Bartashevich, and T. Goto, Singlet ground state and magnetization plateaus in $\text{Ba}_3\text{Mn}_2\text{O}_8$, *J. Phys. Soc. Jpn.* **70**, 1790 (2001).
- [12] M. B. Stone, M. D. Lumsden, S. Chang, E. C. Samulon, C. D. Batista, and I. R. Fisher, Singlet-Triplet Dispersion Reveals Additional Frustration in the Triangular-Lattice Dimer Compound $\text{Ba}_3\text{Mn}_2\text{O}_8$, *Phys. Rev. Lett.* **100**, 237201 (2008).
- [13] Y. Singh and D. C. Johnston, Singlet ground state in the spin-1/2 dimer compound $\text{Ba}_3\text{Cr}_2\text{O}_8$, *Phys. Rev. B* **76**, 012407 (2007).
- [14] H. Tsujii, B. Andraka, M. Uchida, H. Tanaka, and Y. Takano, Specific heat of the $S = 1$ spin-dimer antiferromagnet $\text{Ba}_3\text{Mn}_2\text{O}_8$ in high magnetic fields, *Phys. Rev. B* **72**, 214434 (2005).
- [15] B. Bernu, P. Lecheminant, C. Lhuillier, and L. Pierre, Exact spectra, spin susceptibilities, and order parameter of the quantum Heisenberg antiferromagnet on the triangular lattice, *Phys. Rev. B* **50**, 10048 (1994).
- [16] G. H. Wannier, Antiferromagnetism. The triangular Ising net, *Phys. Rev.* **79**, 357 (1950).
- [17] J. Xing, L. D. Sanjeeva, J. Kim, G. R. Stewart, A. Podlesnyak, and A. S. Sefat, Field-induced magnetic transition and spin fluctuations in the quantum spin-liquid candidate CsYbSe_2 , *Phys. Rev. B* **100**, 220407(R) (2019).
- [18] M. Wildner, Structure of $\text{K}_2\text{Co}_2(\text{SeO}_3)_3$, *Acta Crystallogr. C* **50**, 336 (1994).
- [19] G. M. Sheldrick, Crystal structure refinement with SHELXL, *Acta Crystallogr. Sect. C: Struct. Chem.* **71**, 3 (2015).
- [20] O. V. Dolomanov, L. J. Bourhis, R. J. Gildea, J. A. K. Howard, and H. Puschmann, OLEX2: A complete structure solution, refinement and analysis program, *J. Appl. Crystallogr.* **42**, 339 (2009).
- [21] A. L. Spek, Single-crystal structure validation with the program PLATON, *J. Appl. Crystallogr.* **36**, 7 (2003).
- [22] See Supplemental Material at <http://link.aps.org/supplemental/10.1103/PhysRevB.102.224430> for the crystallographic data including Wyckoff position, atomic coordinates, occupancies, and equivalent isotropic displacement parameters for the studied compound at 100 K.
- [23] M. E. Lines, Magnetic properties of CoCl_2 and NiCl_2 , *Phys. Rev.* **131**, 546 (1963).
- [24] H. Shiba, Y. Ueda, K. Okunishi, S. Kimura, and K. Kindo, Exchange interaction via crystal-field excited states and its importance in CsCoCl_3 , *J. Phys. Soc. Jpn.* **72**, 2326 (2003).
- [25] Y. Shirata, H. Tanaka, A. Matsuo, and K. Kindo, Experimental Realization of a Spin-1/2 Triangular-Lattice Heisenberg Antiferromagnet, *Phys. Rev. Lett.* **108**, 057205(2012).
- [26] H. Liu and G. Khaliullin, Pseudospin exchange interactions in d 7 cobalt compounds: Possible realization of the Kitaev model, *Phys. Rev. B* **97**, 014407 (2018).
- [27] E. C. Samulon, K. A. Al-Hassanieh, Y.-J. Jo, M. C. Shapiro, L. Balicas, C. D. Batista, and I. R. Fisher, Anisotropic phase diagram of the frustrated spin dimer compound $\text{Ba}_3\text{Mn}_2\text{O}_8$, *Phys. Rev. B* **81**, 104421 (2010).
- [28] U. Arjun, V. Kumar, P. K. Anjana, A. Thirumurugan, J. Sichelschmidt, A. V. Mahajan, and R. Nath, Singlet ground state in the spin-1/2 weakly coupled dimer compound $\text{NH}_4[(\text{V}_2\text{O}_3)_2(4,4'\text{-bpy})_2(\text{H}_2\text{PO}_4)(\text{PO}_4)_2]\cdot 0.5\text{H}_2\text{O}$, *Phys. Rev. B* **95**, 174421 (2017).
- [29] R. Zhong, S. Guo, G. Xu, Z. Xu, and R. J. Cava, Strong quantum fluctuations in a quantum spin liquid candidate with a Co-Based triangular lattice, *Proc. Natl. Acad. Sci.* **116**, 14505 (2019).
- [30] R. Zhong, T. Gao, N. P. Ong, and R. J. Cava, Weak-field induced nonmagnetic state in a Co-based honeycomb, *Sci. Adv.* **6**, eaay6953 (2020).

- [31] S. V. Streltsov and D. I. Khomskii, Covalent bonds against magnetism in transition metal compounds, *Proc. Natl. Acad. Sci.* **113**, 10491 (2016).
- [32] C. He, H. Zheng, J. F. Mitchell, M. L. Foo, R. J. Cava, and C. Leighton, Low temperature Schottky anomalies in the specific heat of LaCoO_3 : Defect-stabilized finite spin states, *Appl. Phys. Lett.* **94**, 102514 (2009).
- [33] B. Gao, T. Chen, D. W. Tam, C.-L. Huang, K. Sasmal, D. T. Adroja, F. Ye, H. Cao, G. Sala, M. B. Stone, C. Baines, J. A. T. Verezhak, H. Hu, J.-H. Chung, X. Xu, S.-W. Cheong, M. Nallaiyan, S. Spagna, M. B. Maple, A. H. Nevidomskyy, E. Morosan, G. Chen, and P. Dai, Experimental signatures of a three-dimensional quantum spin liquid in effective spin-1/2 $\text{Ce}_2\text{Zr}_2\text{O}_7$ pyrochlore, *Nat. Phys.* **15**, 1052 (2019).
- [34] K. Sasaki, T. Sugimoto, T. Tohyama, and S. Sota, Magnetic excitations in magnetization plateaus of a frustrated spin ladder, *Phys. Rev. B* **101**, 144407 (2020).
- [35] M. Takigawa, S. Matsubara, M. Horvatić, C. Berthier, H. Kageyama, and Y. Ueda, NMR Evidence for the Persistence of a Spin Superlattice Beyond the 1/8 Magnetization Plateau in $\text{SrCu}_2(\text{BO}_3)_2$, *Phys. Rev. Lett.* **101**, 037202 (2008).
- [36] K. Kodama, M. Takigawa, M. Horvatić, C. Berthier, H. Kageyama, Y. Ueda, S. Miyahara, F. Becca, and F. Mila, Magnetic superstructure in the two-dimensional quantum antiferromagnet $\text{SrCu}_2(\text{BO}_3)_2$, *Science* **298**, 395 (2002).
- [37] E. C. Samulon, Y.-J. Jo, P. Sengupta, C. D. Batista, M. Jaime, L. Balicas, and I. R. Fisher, Ordered magnetic phases of the frustrated spin-dimer compound $\text{Ba}_3\text{Mn}_2\text{O}_8$, *Phys. Rev. B* **77**, 214441 (2008).
- [38] E. C. Samulon, Y. Kohama, R. D. McDonald, M. C. Shapiro, K. A. Al-Hassanieh, C. D. Batista, M. Jaime, and I. R. Fisher, Asymmetric Quintuplet Condensation in the Frustrated $s = 1$ Spin Dimer Compound $\text{Ba}_3\text{Mn}_2\text{O}_8$, *Phys. Rev. Lett.* **103**, 047202 (2009).